Original Article
Determination of binding affinity of molecular imaging agents for steroid hormone receptors in breast cancer

Kelley Salem[1], Manoj Kumar[1], Kyle C Kloepping[1,2], Ciara J Michel[1], Yongjun Yan[1,4], Amy M Fowler[1,3,4]

[1]Department of Radiology, University of Wisconsin School of Medicine and Public Health, 600 Highland Avenue, Madison, WI 53792, USA; [2]Perkin Elmer, Waltham, MA, USA; [3]University of Wisconsin Carbone Cancer Center, 600 Highland Avenue, Madison, WI 53792, USA; [4]Department of Medical Physics, University of Wisconsin School of Medicine and Public Health, 1111 Highland Avenue, Madison, WI 53705, USA

Abstract: 16α-[^{18}F]Fluoro-17β-estradiol ([^{18}F]FES) and 21-[^{18}F]-Fluoro-$16\alpha,17\alpha$-[(R)-(1'-α-furylmethylidene)dioxyl]-19-norpregn-4-ene-3,20-dione ([^{18}F]FFNP) are being investigated as imaging biomarkers for breast cancer patients. Quantitative positron emission tomography (PET) reflects both total receptor content and binding affinity. To study factors that may alter radiopharmaceutical binding and impact PET accuracy, assays that can separate receptor amount from binding affinity are needed. The study purpose was to quantify the binding parameters of [^{18}F]FES and [^{18}F]FFNP in breast cancer. Estrogen receptor-alpha (ER) and progesterone receptor (PR) positive breast cancer cell lines (MCF-7 and T47D) were used to measure [^{18}F]FES and [^{18}F]FFNP binding parameters via saturation and competitive binding curves. The equilibrium dissociation constant (K_d) and total receptor density (B_{max}) were determined using nonlinear regression of the saturation binding curves. Half-maximal inhibitory concentration (IC50) was determined using nonlinear regression of the competitive binding curves. Linear correlation between increasing cell number and tracer uptake was observed for both [^{18}F]FES and [^{18}F]FFNP (R^2=0.99 and 0.91, respectively). Using [^{18}F]FES, the K_d for ER in MCF-7 cells was 0.13 ± 0.02 nM with a B_{max} of 1901 ± 89.3 fmol/mg protein and IC50 of 0.085 nM (95% CI: 0.069-0.104 nM). Using [^{18}F]FFNP, the K_d for PR in T47D cells was 0.41 ± 0.05 nM with a B_{max} of 1984 ± 75.6 fmol/mg protein and IC50 of 2.6 nM (95% CI: 2.0-3.4 nM). The ligand binding function of ER and PR can be quantified using [^{18}F]FES and [^{18}F]FFNP and are comparable to previous studies using tritiated radioligands. [^{18}F]FES and [^{18}F]FFNP can be used in cell-based assays to quantify receptor-radioligand binding affinity, which cannot be obtained from a single PET examination.

Keywords: Estrogen receptor, progesterone receptor, breast cancer, [^{18}F]FES, [^{18}F]FFNP, radioligand binding affinity, equilibrium dissociation constant, K_d

Introduction

Advances in early detection and treatment of breast cancer have led to a steady decrease in mortality, however recurrent and metastatic disease continues to be problematic [1]. The majority of deaths due to breast cancer occur in women with estrogen receptor alpha-positive (ER) disease. Endocrine-based therapies are aimed at directly antagonizing ER function or reducing endogenous estradiol levels. Due to the well-recognized diversity and complexity of ER signaling mechanisms, it is inevitable that some patients will have disease that has circumvented the standard methods for blocking ER function and have become endocrine insensitive [2]. This important shift in receptor functionality cannot be directly measured by current clinical diagnostic approaches.

Functional imaging provides a useful tool for detecting biomarkers with predictive power for therapy response [3]. 16α-[^{18}F]Fluoro-17β-estradiol ([^{18}F]FES) is a radiolabeled estrogen that binds to ER [4, 5]. A recent study showed that [^{18}F]FES binds specifically to the ligand binding domain of ER [6]. Positron emission tomography (PET) imaging coupled with [^{18}F]FES has been studied in patients with ER+ metastatic breast cancer and may be useful for predicting clinical benefit from endocrine therapy [7, 8].

Another biomarker for endocrine sensitivity is the classic estrogen-regulated target gene progesterone receptor (PR) [9, 10]. A radiolabeled progestin, 21-[¹⁸F]-fluoro-16α,17α-[(R)-(1'-α-furylmethylidene)dioxyl]-19-norpregn-4-ene-3,20-dione ([¹⁸F]FFNP), has been developed to image PR [11, 12]. Preclinical data indicate that [¹⁸F]FFNP PET imaging can quantify changes in PR expression and distinguish endocrine-sensitive from endocrine-resistant mouse mammary carcinomas [13, 14]. A small "first-in-human" feasibility study demonstrated that [¹⁸F]FFNP PET imaging of breast cancer patients is safe and can identify PR+ tumors as defined by standard immunohistochemistry [15].

Coupling these investigational radiopharmaceuticals with PET imaging is proving to be useful in the clinical setting [16, 17]. *In vivo* steroid hormone receptor quantification via a standardized uptake value reflects a combination of the amount of receptor protein and the binding affinity of the receptor for the imaging agent (*i.e.* binding potential), as well as pharmacokinetic variables such as plasma protein binding and metabolism of the tracer [18]. To study mechanistic factors that may alter binding of these radiopharmaceuticals and impact the diagnostic accuracy of PET imaging, assays that can separate receptor amount from binding affinity are needed. The purpose of this study was to establish cell-based assays to quantify the radioligand binding parameters of [¹⁸F]FES and [¹⁸F]FFNP for investigating the ligand binding function of steroid hormone receptors in breast cancer.

Materials and methods

Cell culture

Experiments were performed under a protocol approved by the Office of Biological Safety. ER+ MCF-7 cells were obtained from the Mallinckrodt Institute of Radiology Pre-Clinical PET/CT Imaging Facility (Washington University School of Medicine). PR+ T47D cells were obtained from the American Type Culture Collection. Authentication was performed using short tandem repeat analysis. MCF-7 and T47D cells were cultured in Dulbecco's Modified Eagle medium (DMEM; Corning) and Roswell Park Memorial Institute (RPMI; Corning), respectively. Media was supplemented with 10% fetal bovine serum (FBS; Corning) and 1% penicillin/

streptomycin (Gibco). Cells were maintained at 37°C with either 5% or 10% CO_2.

Radiopharmaceuticals

[¹⁸F]FES and [¹⁸F]FFNP were synthesized by the UW-Madison Radiopharmaceutical Production Facility using modifications of previously described methods [14, 19]. Briefly, [¹⁸F]FES was synthesized by adding 1 mg FES precursor, 3-methoxymethyl-16beta,17beta-epiestriol-O-cyclic sulfone (ABX Advanced Biochemical Compounds) in 0.3 mL anhydrous acetonitrile into a vial containing dried mixture of [¹⁸F]fluoride ion, 5 mg Kryptofix® 2.2.2 and 1 mg K_2CO_3. Radiolabeling was performed at 110°C for 10 min. Hydrolysis using 0.1 mL of 1 N HCl and 0.9 mL acetonitrile was conducted at 100°C for 15 min. After neutralization with 0.1 mL of 1 N NaOH and 1 mL 1 N sodium acetate, the crude product was purified with HPLC (high-performance liquid chromatography) with a Luna C18(2) 10 × 250 mm (5 μm) column (Mobile phase: aqueous 50% ethanol solution).

[¹⁸F]FFNP was synthesized by adding 4 mg FFNP precursor, 16α,17α-[(R)-(1'-α-furyl methylidene)dioxyl]-21-[[(methyl)sulfonyl]oxyl]-19-norpregn-4-ene-3,20-dione (ABX Advanced Biochemical Compounds), in 0.6 mL anhydrous acetonitrile into the vial containing dried mixture of [¹⁸F]fluoride ion, 2 mg Kryptofix® 2.2.2 and 0.4 mg K_2CO_3. Radiolabeling was performed at 85°C for 5 min. After mixing with a pre-cooled (5°C) solution of 1 mL acetonitrile and 2 mL H_2O, the crude product was purified with HPLC with a Luna C18(2) 10 X 250 mm (5 μm) column (Mobile phase : aqueous 60% acetonitrile solution).

For both tracers, the HPLC collection was purified with a C18 cartridge to remove trace amount of organic solvents. The purified products were formulated in 0.9% sodium chloride injection containing 10% ethanol injection and sterilized with a sterile, pyrogen-free sterile membrane filter into a 30 mL sterile empty vial.

For [¹⁸F]FES, the radiochemical purity of final product at end of synthesis is >99% and the specific activity exceeded 55.3 GBq/μmol (1495 mCi/μmol). [¹⁸F]FES is stable for 6 hours at the drug strength no more than 14.6 mCi/mL and the radiochemical purity at 6 h post synthesis is >98%. For [¹⁸F]FFNP, the radiochemical purity of the final product at the end of syn-

A
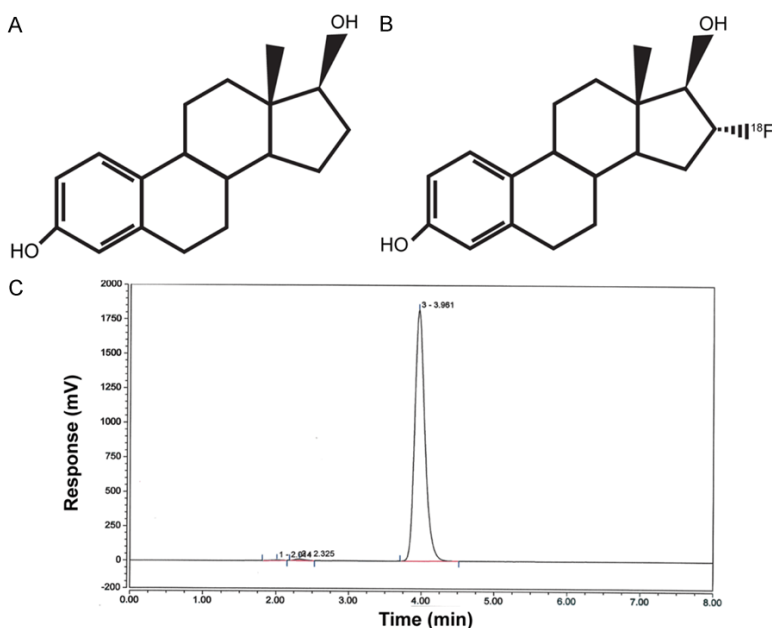
B

C

Figure 1. Chemical structures of 17β-estradiol (A) and [¹⁸F]FES (B). Representative HPLC chromatogram for [¹⁸F]FES (C).

A

B

C

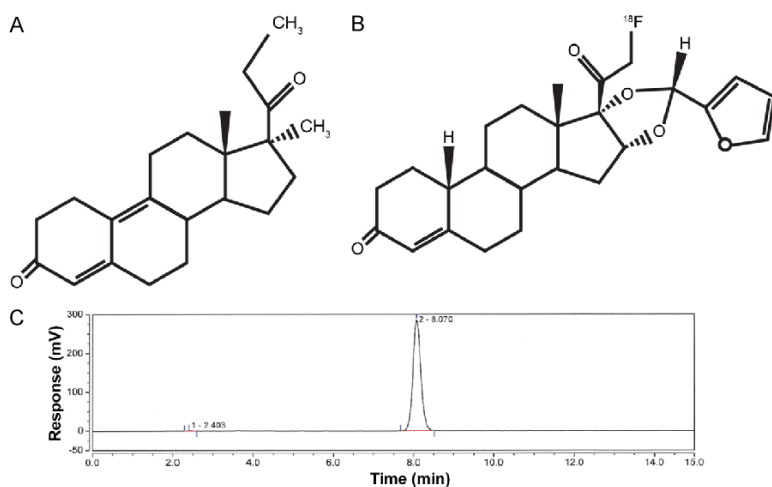**Figure 2.** Chemical structures of promegestone (R5020) (A) and [¹⁸F]FFNP (B). Representative HPLC chromatogram for [¹⁸F]FFNP (C).

a 24-well plate. After adhering overnight, cells were washed with phosphate-buffered saline (PBS) and phenol-free media containing 10% charcoal/dextran stripped FBS, 2% L-glutamine, and 1% penicillin/streptomycin (ss-media) was added to the cells for 24 h. MCF-7 and T47D cells were then incubated with either 0.037 MBq (1 µCi) [¹⁸F]FES or 0.074 MBq (2 µCi) [¹⁸F]FFNP, respectively, for 1 h at 37°C. After the 1 h incubation, cells were washed twice with 0.5 mL PBS. Cells were then lysed in 1 mL 1N NaOH and collected into gamma counter tubes. The wells were then washed twice with 0.5 mL PBS and each wash was added to the same tube as the cell lysate (2 mL final total volume). Radioactivity was measured with a gamma counter (2480 Wizard², Perkin Elmer) and data was background- and decay-corrected.

For saturation binding assays, MCF-7 or T47D cells (1 × 10⁵) were plated in two 24-well plates. The next day, cells were washed with PBS and placed in ss-media. Immediately prior to tracer addition, one plate was treated with ethanol (EtOH) control and the other treated with either 1 × 10⁻⁸ M 17β-estradiol (E2; Sigma) or 2 × 10⁻⁷ M promegestone (R5020; Perkin Elmer), a synthetic progestin. Increasing concentrations of tracer, 0.002-0.22 MBq (0.06-6 µCi) [¹⁸F]FES or 0.004-0.42 MBq (0.11-11.4 µCi) [¹⁸F]FFNP, were then administered to the plates. After incubation for 1 h at 37°C, cells were harvested and radioactivity measured as above. A standard curve was prepared using the same tracer concentrations diluted in 2 mL PBS and radioactivity counted with the cell lysates. The tracer concentration (x-axis) was calculated from the specific activity (mCi/µmol) and administered

thesis is >99% with the specific activity exceeding 74 GBq/µmol (2000 mCi/µmol). [¹⁸F]FFNP is stable for 6 hours at the drug strength no more than 6 mCi/mL and the radiochemical purity at 6 h post synthesis is >97%. Chemical structures and representative HPLC chromatograms of [¹⁸F]FES and [¹⁸F]FFNP are shown in **Figures 1** and **2**, respectively.

[¹⁸F]FES and [¹⁸F]FFNP binding assays

For linearity assays, cells were serially diluted 1:2 from 1.50 × 10⁵ to 4.688 × 10³ per well in
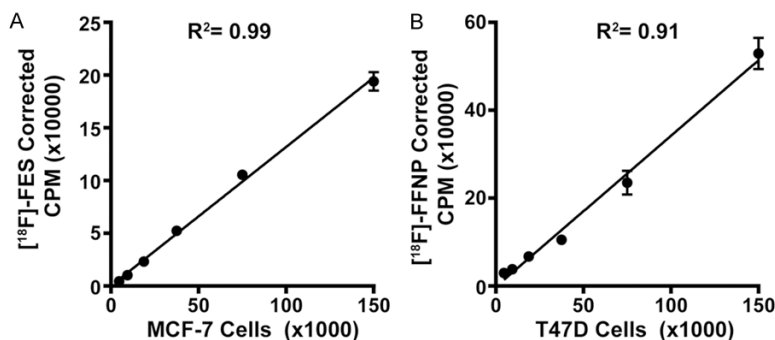
Figure 3. [¹⁸F]FES and [¹⁸F]FFNP uptake correlates with increasing cell number. Steroid hormone deprived ER+ MCF-7 (A) and PR+ T47D (B) cells were seeded with increasing cell numbers in 24-well plates and treated with 0.037 MBq (1 µCi) [¹⁸F]FES or 0.074 MBq (2 µCi) [¹⁸F]FFNP for 1 h, respectively. Counts per minute (CPM) were background- and decay-corrected. Data shown (mean±standard error) are representative from three independent experiments performed in triplicate.
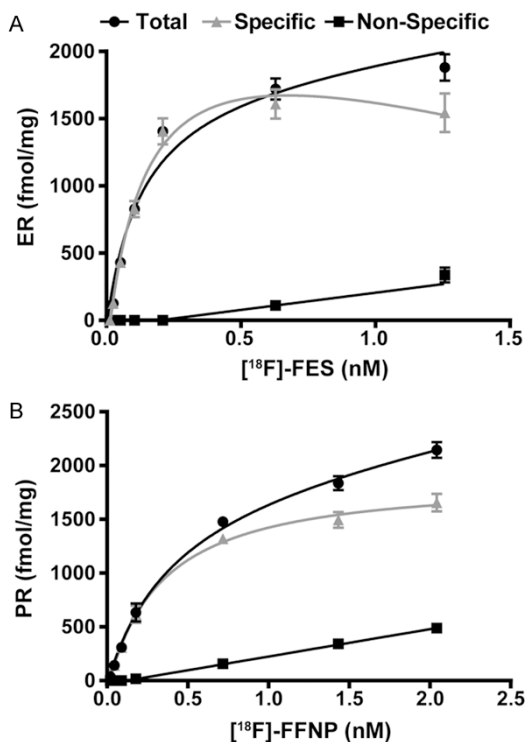

Figure 4. Saturation binding curves yield K_d and B_{max} for [¹⁸F]FES and [¹⁸F]FFNP. Steroid hormone deprived ER+ MCF-7 (A) and PR+ T47D (B) cells were seeded in identical 24-well plates treated with 0.002-0.22 MBq (0.06-6 µCi) [¹⁸F]FES and 0.004-0.42 MBq (0.11-11.4 µCi) [¹⁸F]FFNP for 1 h, respectively. Total binding, non-specific, and specific binding (total binding minus non-specific binding) are shown. Values represent the mean ± standard error of three independent experiments performed in triplicate.

dose (µCi). The receptor amount (y-axis) was calculated from the standard curve and nor-malized to total protein per well (fmol receptor/mg protein). Total protein was measured using Bradford dye reagent (Bio-Rad). The equilibrium dissociation constant (K_d) and total receptor density (B_{max}) were determined using nonlinear regression (binding one site-total and nonspecific binding) with GraphPad Prism 6.05 software.

For competitive binding assays, cells were plated at a density of 1×10^5 per well in 24-well plates. The next day, cells were washed with PBS and placed in ss-media. Immediately prior to tracer addition, cells were treated with either EtOH or increasing amounts of cold hormone. For the [¹⁸F]FES competitive binding assay, MCF-7 cells were treated with 1×10^{-8} to 1×10^{-13} M E2. For the [¹⁸F]FFNP competitive binding assay, T47D cells were treated with 1×10^{-7} to 1×10^{-12} M R5020. MCF-7 cells were then incubated with 0.037 MBq (1 µCi) [¹⁸F]FES and T47D cells with 0.074 MBq (2 µCi) [¹⁸F]FFNP for 1 h at 37°C. Cells were harvested and radioactivity measured as above. Data is shown as percent maximum uptake values (samples containing tracer with no cold hormone added =100%). Half-maximal inhibitory concentration (IC50) was determined using nonlinear regression (dose response-inhibition) with GraphPad Prism.

Results

Using ER+ MCF-7 and PR+ T47D breast cancer cell lines, we found good linear correlation between increasing cell number and tracer uptake for both [¹⁸F]FES and [¹⁸F]FFNP (R^2=0.99 and 0.91, respectively; **Figure 3**). The minimum number of cells used in the linearity assays (~4,700) showed detectable tracer uptake above background (mean ± standard error background-corrected CPM 4,438±392 for [¹⁸F]FES and 29,759±2,686 for [¹⁸F]FFNP).

The quantitative binding parameters of [¹⁸F]FES and [¹⁸F]FFNP (K_d, B_{max}, and IC50) determined by saturation (**Figure 4**) and competitive binding curves (**Figure 5**) are summarized in **Table 1**. The K_d value determined using [¹⁸F]FES in
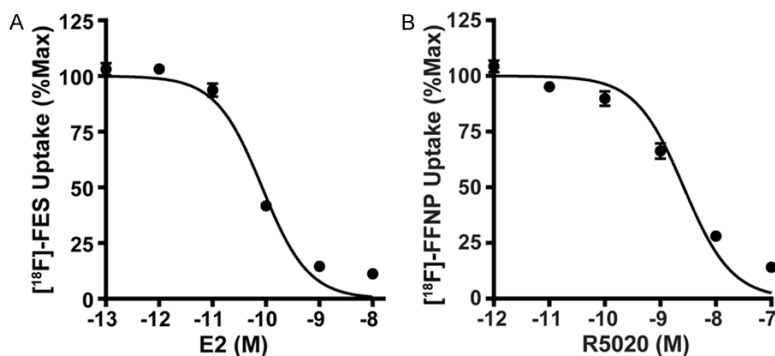
Figure 5. Competitive binding curves yield IC50 values. Steroid hormone deprived ER+ MCF-7 (A) and PR+ T47D (B) cells were treated with either cold E2 (10^{-8}-10^{-13} M) or cold R5020 (10^{-7}-10^{-12} M) just prior to the addition of 0.037 MBq (1 µCi) [^{18}F]FES or 0.074 MBq (2 µCi) [^{18}F]FFNP, respectively. Percent maximum uptake value was calculated by normalizing background- and decay-corrected counts per minute to wells containing [^{18}F]FES or [^{18}F]FFNP with no cold hormone. Values represent the mean±standard error of three independent experiments performed in triplicate.

maceuticals and impact the quantitative accuracy of PET imaging, assays that can separate receptor amount from binding affinity are needed. The goal of this study was to establish cell-based assays using [^{18}F]FES and [^{18}F]FFNP for quantifying the ligand binding function of ER and PR. Using saturation and competitive binding assays, we measured K_d and B_{max} as well as the IC50 values of representative ligand agonists (17β-estradiol and the synthetic progestin, R5020). The ligand binding functions of ER and PR quantified using [^{18}F]FES and [^{18}F]FFNP were generally comparable to historical studies using tritiated steroid hormones.

MCF-7 cells was 0.13 nM, which is within the range of equilibrium dissociation constants reported using [^{3}H]estradiol (0.06 to 0.226 nM) [20-22]. The B_{max} value determined using [^{18}F]FES was 1,901 fmol/mg protein, which also falls within the wide range of ER protein content in MCF-7 cells (100 to 10,000 fmol/mg protein) measured by [^{3}H]estradiol or Western blot analysis [20, 23-25]. Prior studies using [^{3}H]R5020 have reported equilibrium dissociation constants for PR ranging from 0.40 to 3.57 nM [26-29], which is similar to the K_d of 0.41 nM using [^{18}F]FFNP. The B_{max} of PR in T47D cells was 1,984 fmol/mg protein using [^{18}F]FFNP, which is slightly higher than published PR concentrations ranging from 254 to 1,221 fmol/mg protein using [^{3}H]R5020 [28, 30]. IC50 values determined by competing [^{18}F]FES binding to ER with cold E2 corresponded closer to its equilibrium dissociation constant than the IC50 values determined by competing [^{18}F]FFNP binding to PR with cold R5020.

Discussion

[^{18}F]FES and [^{18}F]FFNP are being investigated as predictive and pharmacodynamic biomarkers for response to endocrine therapy in breast cancer patients using PET imaging [7]. Standardized uptake values (SUV) obtained from attenuation-corrected PET images reflect both total receptor content (B_{max}) and binding affinity ($1/K_d$) [18]. To study mechanistic factors that may alter binding of these radiophar-

These results indicate that [^{18}F]-labeled steroid hormone radioligands can be used in cell-based assays to quantify receptor-radioligand binding affinity, which cannot be obtained from a single PET imaging examination. As proof-of-principle, the investigation focused on the most widely used and well-characterized steroid hormone receptor positive human breast cancer cell lines, MCF-7 and T47D [31]. To the best of our knowledge, K_d values for [^{18}F]FES and [^{18}F]FFNP have not been previously reported. Prior investigations into the binding affinity of [^{18}F]FES used *ex vivo* biochemical competitive radiometric binding assays with [^{3}H]estradiol and purified receptor protein or homogenates of steroid hormone receptor rich tissue, such as rat uteri, to calculate relative binding affinity (RBA) [4, 5]. Similarly for [^{18}F]FFNP, previous reports used [^{3}H]R5020 and purified PR protein or rat uterine homogenates to calculate RBA [27, 32]. Our results advance the existing literature by providing specific measurements of binding affinity in the important context of intact, viable cells.

For comparison, the *in vivo* assessment of ER binding in MCF-7 xenograft tumors using [^{18}F]FES PET imaging has been previously reported by our research group and others [6, 33]. In the study by Salem *et al*, PET imaging performed 1 hour after injection of 9.25 MBq (250 µCi) [^{18}F]

Table 1. Binding Parameters of [^{18}F]FES and [^{18}F]FFNP

Cell Line/Tracer	K_d (nM)	95% CI (nM)	B_{max} (fmol/mg)	95% CI (fmol/mg)	R^2	IC50 (nM)	95% CI (nM)	R^2
MCF-7 [^{18}F]FES	0.13±0.02	0.09-0.17	1901±89.3	1723-2079	0.93	0.085	0.069-0.104	0.96
T47D [^{18}F]FFNP	0.41±0.05	0.31-0.50	1984±75.6	1833-2134	0.98	2.645	2.037-3.436	0.92

FES demonstrated 3.0±0.41 percent mean injected dose per gram (%ID/g) and 7.2±0.60 tumor-to-muscle ratio in MCF-7 xenografts grown in female athymic nude mice [6]. Heidari *et al* performed PET imaging of MCF-7 tumor bearing nude mice approximately 1 hour after intravenous injection with 9.7 MBq (260 µCi) [^{18}F]FES and found that the mean standardized uptake value (SUV$_{mean}$) was 0.33±0.02 with a tumor-to-blood ratio of 4.17±0.41 [33]. To the best of our knowledge, no previous reports of the *in vivo* assessment of PR binding using [^{18}F]FFNP in T47D xenograft tumors have been published.

There are several potential applications of this work. New radiopharmaceuticals continue to be developed for steroid hormone receptor imaging [27, 34, 35]. Comparison of the binding parameters of new radiotracers with [^{18}F]FES and [^{18}F]FFNP as reference standards may give insight into their potential for further clinical utility in patients. Also of interest is determining how recently identified somatic hot-spot mutations occurring in the ligand binding domain of ER in patients with endocrine-resistant metastatic breast cancer impact the binding affinity of [^{18}F]FES [36]. Lastly, [^{18}F]FES and [^{18}F]FFNP binding assays can potentially be modified to a smaller scale to investigate receptor status and ligand binding function of *ex vivo* patient samples obtained from serial liquid biopsies such as pleural effusions, ascites, and circulating tumor cells when quantification via PET imaging may be challenging.

Disclosure of conflict of interest

None.

Address correspondence to: Dr. Amy M Fowler, Department of Radiology, University of Wisconsin, 600 Highland Avenue, Madison, WI 53792-3252, USA. Tel: 608-262-9186; Fax: 608-265-1836; E-mail: afowler@uwhealth.org

References

[1] Jatoi I, Chen BE, Anderson WF and Rosenberg PS. Breast cancer mortality trends in the United States according to estrogen receptor status and age at diagnosis. J Clin Oncol 2007; 25: 1683-1690.

[2] Osborne CK and Schiff R. Mechanisms of endocrine resistance in breast cancer. Annu Rev Med 2011; 62: 233-247.

[3] Mankoff DA, Pryma DA and Clark AS. Molecular imaging biomarkers for oncology clinical trials. J Nucl Med 2014; 55: 525-528.

[4] Kiesewetter DO, Kilbourn MR, Landvatter SW, Heiman DF, Katzenellenbogen JA and Welch MJ. Preparation of four fluorine-18-labeled estrogens and their selective uptakes in target tissues of immature rats. J Nucl Med 1984; 25: 1212-1221.

[5] Yoo J, Dence CS, Sharp TL, Katzenellenbogen JA and Welch MJ. Synthesis of an estrogen receptor beta-selective radioligand: 5-[18F]fluoro-(2R,3S)-2,3-bis(4-hydroxyphenyl)pentanenitrile and comparison of in vivo distribution with 16alpha-[18F]fluoro-17beta-estradiol. J Med Chem 2005; 48: 6366-6378.

[6] Salem K, Kumar M, Powers GL, Jeffery JJ, Yan Y, Mahajan AM and Fowler AM. (18)F-16alpha-17beta-Fluoroestradiol binding specificity in estrogen receptor-positive breast cancer. Radiology 2018; 286: 856-864.

[7] Fowler AM, Clark AS, Katzenellenbogen JA, Linden HM and Dehdashti F. Imaging diagnostic and therapeutic targets: steroid receptors in breast cancer. J Nucl Med 2016; 57 Suppl 1: 75s-80s.

[8] van Kruchten M, de Vries EG, Brown M, de Vries EF, Glaudemans AW, Dierckx RA, Schroder CP and Hospers GA. PET imaging of oestrogen receptors in patients with breast cancer. Lancet Oncol 2013; 14: e465-475.

[9] Osborne CK, Yochmowitz MG, Knight WA 3rd and McGuire WL. The value of estrogen and progesterone receptors in the treatment of breast cancer. Cancer 1980; 46: 2884-2888.

[10] Howell A, Harland RN, Barnes DM, Baildam AD, Wilkinson MJ, Hayward E, Swindell R and Sellwood RA. Endocrine therapy for advanced carcinoma of the breast: relationship between the effect of tamoxifen upon concentrations of progesterone receptor and subsequent response to treatment. Cancer Res 1987; 47: 300-304.

[11] Buckman BO, Bonasera TA, Kirschbaum KS, Welch MJ and Katzenellenbogen JA. Fluorine-18-labeled progestin 16 alpha, 17 alpha-dioxolanes: development of high-affinity ligands for the progesterone receptor with high in vivo target site selectivity. J Med Chem 1995; 38: 328-337.

[12] Vijaykumar D, Mao W, Kirschbaum KS and Katzenellenbogen JA. An efficient route for the preparation of a 21-fluoro progestin-16 alpha,17 alpha-dioxolane, a high-affinity ligand for PET imaging of the progesterone receptor. J Org Chem 2002; 67: 4904-4910.

[13] Chan SR, Fowler AM, Allen JA, Zhou D, Dence CS, Sharp TL, Fettig NM, Dehdashti F and Katzenellenbogen JA. Longitudinal noninvasive imaging of progesterone receptor as a predictive biomarker of tumor responsiveness to estrogen deprivation therapy. Clin Cancer Res 2015; 21: 1063-1070.

[14] Fowler AM, Chan SR, Sharp TL, Fettig NM, Zhou D, Dence CS, Carlson KE, Jeyakumar M, Katzenellenbogen JA, Schreiber RD and Welch MJ. Small-animal PET of steroid hormone receptors predicts tumor response to endocrine therapy using a preclinical model of breast cancer. J Nucl Med 2012; 53: 1119-1126.

[15] Dehdashti F, Laforest R, Gao F, Aft RL, Dence CS, Zhou D, Shoghi KI, Siegel BA, Katzenellenbogen JA and Welch MJ. Assessment of progesterone receptors in breast carcinoma by PET with 21-18F-fluoro-16alpha,17alpha-[(R)-(1'-alpha-furylmethylidene)dioxy]-19-norpregn-4-ene-3,20-dione. J Nucl Med 2012; 53: 363-370.

[16] van Kruchten M, Glaudemans AW, de Vries EF, Beets-Tan RG, Schroder CP, Dierckx RA, de Vries EG and Hospers GA. PET imaging of estrogen receptors as a diagnostic tool for breast cancer patients presenting with a clinical dilemma. J Nucl Med 2012; 53: 182-190.

[17] Venema CM, Apollonio G, Hospers GA, Schroder CP, Dierckx RA, de Vries EF and Glaudemans AW. Recommendations and technical aspects of 16alpha-[18F]fluoro-17beta-estradiol PET to image the estrogen receptor in vivo: the Groningen experience. Clin Nucl Med 2016; 41: 844-851.

[18] Mintun MA, Raichle ME, Kilbourn MR, Wooten GF and Welch MJ. A quantitative model for the in vivo assessment of drug binding sites with positron emission tomography. Ann Neurol 1984; 15: 217-227.

[19] Zhou D, Lin M, Yasui N, Al-Qahtani MH, Dence CS, Schwarz S and Katzenellenbogen JA. Optimization of the preparation of fluorine-18-labeled steroid receptor ligands 16alpha-[18F]fluoroestradiol (FES), [18F]fluoro furanyl norprogesterone (FFNP), and 16beta-[18F]fluoro-5alpha-dihydrotestosterone (FDHT) as radiopharmaceuticals. J Labelled Comp Radiopharm 2014; 57: 371-377.

[20] Horwitz KB, Costlow ME and McGuire WL. MCF-7; a human breast cancer cell line with estrogen, androgen, progesterone, and glucocorticoid receptors. Steroids 1975; 26: 785-795.

[21] Nawata H, Chong MT, Bronzert D and Lippman ME. Estradiol-independent growth of a subline of MCF-7 human breast cancer cells in culture. J Biol Chem 1981; 256: 6895-6902.

[22] Olea-Serrano N, Devleeschouwer N, Leclercq G and Heuson JC. Assay for estrogen and progesterone receptors of breast cancer cell lines in monolayer culture. Eur J Cancer Clin Oncol 1985; 21: 965-973.

[23] Pais A and Degani H. Estrogen receptor-targeted contrast agents for molecular magnetic resonance imaging of breast cancer hormonal status. Front Oncol 2016; 6: 100.

[24] Faye JC, Toulas C and Bayard F. Differential estrogenic responsiveness of MCF-7 cells. Relationship to the presence of two different estrogen receptors. J Recept Res 1989; 9: 203-219.

[25] Martin MB, Reiter R, Pham T, Avellanet YR, Camara J, Lahm M, Pentecost E, Pratap K, Gilmore BA, Divekar S, Dagata RS, Bull JL and Stoica A. Estrogen-like activity of metals in MCF-7 breast cancer cells. Endocrinology 2003; 144: 2425-2436.

[26] Sarup JC, Rao KV and Fox CF. Decreased progesterone binding and attenuated progesterone action in cultured human breast carcinoma cells treated with epidermal growth factor. Cancer Res 1988; 48: 5071-5078.

[27] Lee JH, Zhou HB, Dence CS, Carlson KE, Welch MJ and Katzenellenbogen JA. Development of

[F-18]fluorine-substituted Tanaproget as a progesterone receptor imaging agent for positron emission tomography. Bioconjug Chem 2010; 21: 1096-1104.

[28] Keydar I, Chen L, Karby S, Weiss FR, Delarea J, Radu M, Chaitcik S and Brenner HJ. Establishment and characterization of a cell line of human breast carcinoma origin. Eur J Cancer 1979; 15: 659-670.

[29] Mockus MB, Lessey BA, Bower MA and Horwitz KB. Estrogen-insensitive progesterone receptors in a human breast cancer cell line: characterization of receptors and of a ligand exchange assay. Endocrinology 1982; 110: 1564-1571.

[30] Horwitz KB, Zava DT, Thilagar AK, Jensen EM and McGuire WL. Steroid receptor analyses of nine human breast cancer cell lines. Cancer Res 1978; 38: 2434-2437.

[31] Burdall SE, Hanby AM, Lansdown MR and Speirs V. Breast cancer cell lines: friend or foe? Breast Cancer Res 2003; 5: 89-95.

[32] Brandes SJ and Katzenellenbogen JA. Fluorinated androgens and progestins: molecular probes for androgen and progesterone receptors with potential use in positron emission tomography. Mol Pharmacol 1987; 32: 391-403.

[33] Heidari P, Deng F, Esfahani SA, Leece AK, Shoup TM, Vasdev N and Mahmood U. Pharmacodynamic imaging guides dosing of a selective estrogen receptor degrader. Clin Cancer Res 2015; 21: 1340-1347.

[34] Wu X, You L, Zhang D, Gao M, Li Z, Xu D, Zhang P, Huang L, Zhuang R, Wu H and Zhang X. Synthesis and preliminary evaluation of a (18) F-labeled ethisterone derivative [(18) F]EAEF for progesterone receptor targeting. Chem Biol Drug Des 2017; 89: 559-565.

[35] Paquette M, Lavallee E, Phoenix S, Ouellet R, Senta H, van Lier JE, Guerin B, Lecomte R and Turcotte EE. Improved estrogen receptor assessment by PET using the novel radiotracer 4FMFES in ER+ breast cancer patients: an ongoing phase II clinical trial. J Nucl Med 2018; 59: 197-203.

[36] Salem K, Kumar M, Michel C, Yan Y and Fowler A. Impact of gain-of-function estrogen receptor alpha gene mutations on 18F-fluoroestradiol binding affinity. J Nucl Med 2017; 58: 1029.